Synthesis, characterization and photovoltaic properties of poly(thiophenevinylene-*alt*-benzobisoxazole)s†‡

Jared F. Mike,[a] Kanwar Nalwa,[b] Andrew J. Makowski,[a] Daniel Putnam,[b] Aimée L. Tomlinson,[c] Sumit Chaudhary[b] and Malika Jeffries-EL*[a]

Received 26th April 2010, Accepted 21st October 2010
DOI: 10.1039/c0cp00353k

Herein we report the synthesis of two solution processible, conjugated polymers containing the benzobisoxazole moiety. The polymers were characterized using ^{1}H NMR, UV-Vis and fluorescence spectroscopy. Thermal gravimetric analysis shows that the polymers do not exhibit significant weight loss until approximately 300 °C under nitrogen. Cyclic voltammetry shows that the polymers have reversible reduction waves with estimated LUMO levels at −3.02 and −3.10 eV relative to vacuum and optical bandgaps of 2.04–2.17 eV. Devices based on blends of the copolymers and [6,6]-phenyl C61 butyric acid methyl ester (PCBM) exhibited modest power conversion efficiencies. Theoretical models reveal that there is poor electron delocalization along the polymer backbone, leading to poor performance. However, the energy levels of these polymers indicate that the incorporation of benzobisoxazoles into the polymer backbone is a promising strategy for the synthesis of new materials.

Introduction

The direct conversion of sunlight into energy using photovoltaic cells (PVC)s has been recognized as an essential component of future global energy production. As a result of their optical and electronic properties, conjugated organic materials are sought after to replace inorganic materials in PVCs. This is due to the many attractive features of organic materials, such as the ability to tune their electron properties for specific applications through chemical synthesis and the simplicity of processing using solution-based techniques.[1,2] One current challenge in the field is the development of conjugated polymers with high electron affinity and/or low band gaps for use in bulk heterojunction PVCs.[3] High electron affinity can reduce the energy loss during the transfer of electrons from the donor to [6,6]-phenyl C61 butyric acid methyl ester (PCBM), a widely used electron acceptor, increasing the output power of the PVC.[4–6] Similarly, low band gap allows for the absorption of photons at longer wavelengths, increasing the percentage of solar energy that can be harvested.[7,8] Currently, a popular design strategy for the manipulation of the energy levels of conjugated polymers is the synthesis of so-called D–A donating (D) and electron-accepting (A) moieties.[9] In these polymers, which are composed of alternating electron donating and electron accepting moieties, the hybridization of the LUMO from the accepting moiety and the HOMO from the donor moiety can be used to reduce the polymers band gap and/or vary its energy levels.[9–11]

Poly(3-alkylthiophene)s are widely studied due to their excellent thermal and environmental stability, high hole mobility, and solution processibility.[12,13] Accordingly, electron-rich alkylthiophenes have been widely used as donor moieties in D–A polymer architectures.[11,14–16] Fully conjugated rigid-rod polybenzobisoxazoles (PBBO)s are multifunctional materials widely known for their excellent tensile strength, thermal stability,[17,18] efficient electron transport,[19,20] photoluminescence,[21–27] and high electron affinity.[21,28–31] Thus the incorporation of the benzobisoxazole (BBO) moiety into D–A polymer architectures is beneficial due to its high electron affinity.[16] Despite these advantageous properties, the use of PBBOs has been limited, largely due to their poor solubility, which requires PBBOs to be processed from acidic solutions. Furthermore, the harsh reaction conditions for the synthesis of PBBOs prevent their derivatization.[18,31–36] To realize the untapped potential of the BBO moiety for the development of novel conjugated polymers, we recently developed an alternative approach toward BBO synthesis using mild conditions.[37] As a result, we can now synthesize soluble PBBO by copolymerizing them with aryl monomers bearing flexible side-chains.[37,38]

Herein we report the synthesis of two new polymers, namely poly[(3,4-didodecylthiopene vinylene)-*alt*-benzo[1,2-*d*;5,4-*d*′]-bisoxazole]-2,6-diyl (PTV*c*BBO) and poly[(3,4-didodecylthiopene vinylene)-*alt*-benzo[1,2-*d*;4,5-*d*′]bisoxazole]-2,6-diyl (PTV*t*BBO). The unique combination of the BBO, thiophene, and vinylene moieties greatly enhances the properties of the resultant polymer by: (1) incorporating vinylene linkages to minimize steric interactions between consecutive aromatic rings, reducing the band gap further;[39–41] (2) increasing rotational freedom of the polymer backbone, improving the polymer's solubility; and (3) adding alkyl side chains along the polymer backbone to increase the solubility significantly.

[a] *Department of Chemistry, Iowa State University, Ames, IA 50011, USA. E-mail: malikaj@iastate.edu; Fax: +1 515-294-0105*
[b] *Department of Electrical Engineering, Iowa State University, Ames, IA 50011, USA*
[c] *Department of Chemistry, North Georgia College & State University, GA 30597, USA*

† Electronic supplementary information (ESI) available: AFM images, Raman spectra, current/voltage characteristics and TGA curves. See DOI: 10.1039/c0cp00353k

‡ The band diagram that is shown in the graphical abstract uses HOMO and LUMO values for PCBM from ref. 4.

Results and discussions

Polymer synthesis and physical characterization

The synthesis of PTV*c*BBO and PTV*t*BBO is shown in Scheme 1. The robust BBOs were stable under basic conditions, allowing for their polymerization using the Horner–Wadsworth–Emmons (HWE) reaction. These reaction conditions were selected because the HWE reaction is known to produce polymers with all *trans*-double bonds. This method also prevents cross-linking, incomplete double bond formation, and other undesirable structural defects. The optimum reaction conditions were to dissolve both 3,4-didodecyl-2,5-thiophenedicarboxaldehyde[42] and a BBO monomer[37] in THF under an inert atmosphere, then add 2.2 equivalents of potassium *tert*-butoxide, and stir the reaction at room temperature for 3 days. Using these conditions the polymers were obtained in satisfactory yields, after removing the low molecular weight material *via* Soxhlet extraction. Both polymers were highly soluble in standard organic solvents, such as THF, *m*-cresol and chloroform at room temperature, facilitating characterization using ^{1}H NMR spectroscopy and gel permeation chromatography (GPC). The ^{1}H NMR spectra for both polymers were in agreement with the proposed polymer structures. The weight-averaged molecular weights (M_w) of the polymers were good in both cases, with monomodal weight distributions. Thermogravimetric analysis revealed that both polymers were thermally stable with 5% weight loss onsets occurring at approximately 300 °C under air. The results are summarized in Table 1.

Optical properties

The photophysical characteristics of the polymers were evaluated by UV-vis absorption and fluorescence spectroscopy both as dilute solutions in THF and thin films. The normalized absorbance and emission spectra for the polymers in solutions and thin films are shown in Fig. 1 and the data are summarized in Table 2. In solution, the UV-vis spectra of both polymers have a single broad absorbance bands, whereas the thin film absorbance spectra for both polymers are slightly broader. The absorption maximum for PTV*t*BBO was red-shifted by 27 nm relative to the absorbance maximum for PTV*c*BBO.

Table 1 Molecular weights and thermal properties of the PTVBBOs

	Yield (%)	M_w[a]	M_w/M_n	T_d[b]/°C
PTV*c*BBO	78	13 400	2.4	303
PTV*t*BBO	87	10 800	2.7	298

[a] Molecular weights and polydispersity indexes determined by GPC *versus* polystyrene standards using THF as the eluent. [b] Temperature at which 5% weight loss is observed by TGA under N_2 with a heating rate of 10 °C min^{-1}.

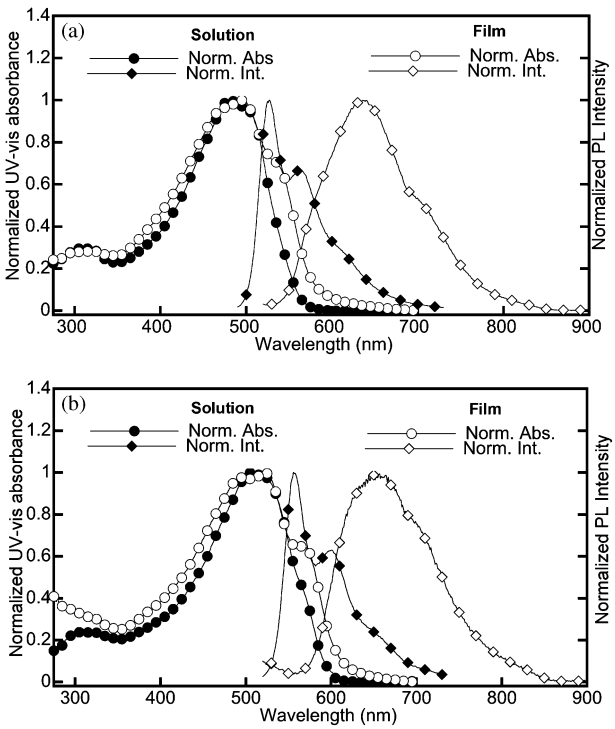

Fig. 1 UV-vis absorption and PL spectra of a: PTV*c*BBO (top) and b: PTV*t*BBO (bottom) in THF and as films spun from THF.

In both cases the UV-vis spectra did not exhibit a second low energy peak typically associated with intramolecular charge-transfer (ICT) transitions within D–A copolymers.[43,44]

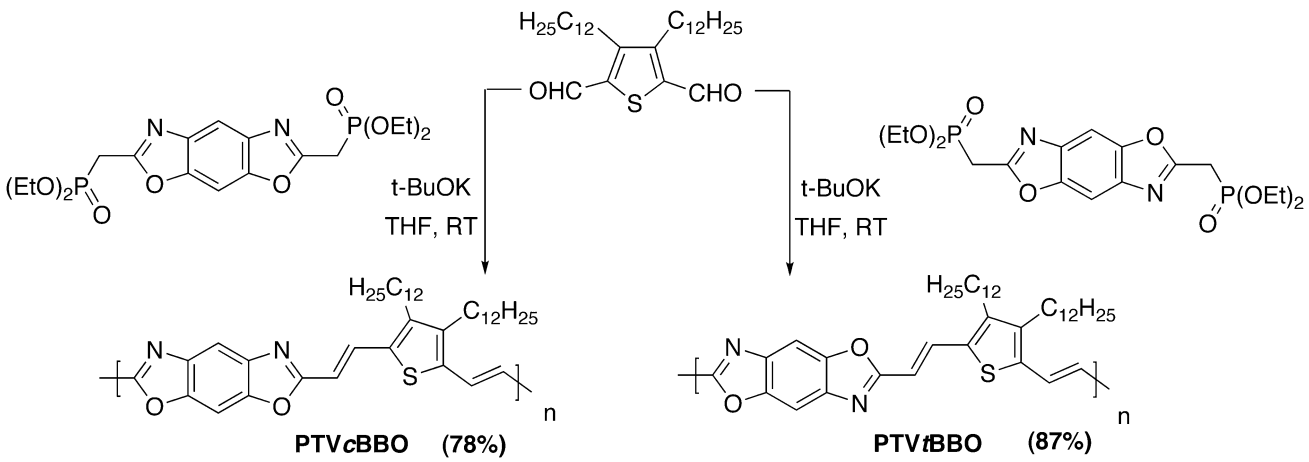

Scheme 1 Synthesis of PTV*c*BBO and PTV*t*BBO.

Table 2 Electronic and optical and electronic properties of PTV*c*BBO and PTV*t*BBO

	Solution					Film			
Polymer	λ_{abs}/nm	λ_{em}/nm	λ_{abs}/nm	λ_{em}/nm	λ_{onset}/nm	$E_g^{opt\,a}$/eV	$E_{onset}^{red\,b}$/eV	LUMO[c]	HOMO[d]
PTV*c*BBO	480	497 (536)	527 (562)	635	571	2.17	−1.34	−3.02	−5.19
PTV*t*BBO	507	525 (565)	556 (601)	653	608	2.04	−1.26	−3.10	−5.14

[a] Estimated from the optical absorption edge. [b] Onset reduction potentials (*vs.* Fc). [c] LUMO = E_{onset}^{red} + 4.8 (eV). [d] HOMO = LUMO − E_g^{opt} (eV).

The optical band gaps for the polymers were estimated from absorption onsets and are summarized in Table 2. In solution the photoluminescence spectra of both polymers exhibit vibrational structure in the form of additional low energy bands. As with the UV-vis spectra the emission spectra of the PTV*t*BBO are red-shifted relative to the PTV*c*BBO. As films, the emission spectra of the polymer thin films were considerably red-shifted, relative to the corresponding solution spectra. This phenomenon is most likely caused by π-stacking and excimer emission. When the polymers were mixed with PCBM, the fluorescence was quenched, suggesting efficient charge transfer between the two materials.

Electrochemical properties

The electrochemical properties of the polymers were investigated by cyclic voltammetry (CV). The data were obtained from polymer thin films on a platinum working electrode, in acetonitrile, using 0.1 M Bu_4NPF_6 as the electrolyte and an Ag/Ag^+ reference electrode. The onsets were referenced to Fc/Fc^+. The CV curves are shown in Fig. 2 and the results are summarized in Table 2. Both polymers exhibited fully chemically reversible reduction waves, whereas oxidation waves were not observed for either polymer. Taking −4.8 eV as the ferrocene energy level relative to vacuum,[44] we estimated the LUMO levels for the polymers (Table 2). Since oxidation onsets could not be measured for the polymers, the highest occupied molecular orbital (HOMO) values were calculated using the optical band gaps and the LUMO levels. Previously we reported band gaps of 2.2–2.4 eV for poly(2,5-bisdodecyloxyphenylenevinylene-*co*-benzobisoxazole)s.[38] Switching the dialkoxybenzenes for the more electron-rich thiophenes changes the position of the HOMO, resulting in a decrease in the bandgap of the polymer.

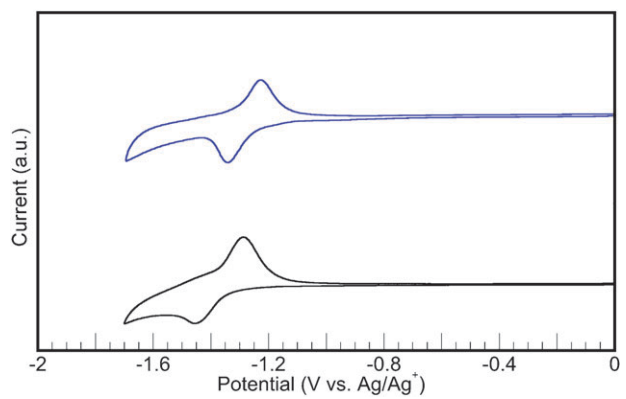

Fig. 2 Cyclic voltammogram of the PTV*c*BBO (bottom) and PTV*t*BBO (top) thin films on platinum electrodes with a scan rate of 50 mV s^{-1}.

Photovoltaic properties

The chemically reversible reduction waves in the cyclic voltammetry suggested that the PTVBBOs could be used as acceptor materials in PVCs with regioregular poly(3-hexylthiophene) (rr-P3HT), one of the most widely studied conjugated polymers.[12,13] However the generally accepted minimum difference between the LUMO levels of the donor and the acceptor is ∼0.4 eV.[45,46] Since rr-P3HT has a LUMO of approximately −3.0 eV,[4,47–49] the LUMO values of −3.02 and −3.10 eV for PTV*c*BBO and PTV*t*BBO, respectively, were insufficient to facilitate efficient electron transfer. However, the energy levels of these polymers suggest that they would be suitable candidates for use in bulk heterojunction PVCs with PCBM. We fabricated such PVCs from (1 : 1) PTVBBO:PCBM blends, using both PTV*c*BBO and PTV*t*BBO. We selected *o*-dichlorobenzene (*o*-DCB) as the solvent due to its high boiling point, which previously has resulted in better self-organization of conjugated polymers, enhancing the performance of PVCs.[50–52] Fig. 3 shows the current–voltage (*I*–*V*) characteristics of our devices under illumination of 100 mW cm^{-2}. For both polymers the open circuit voltages were comparable, 0.35 V and 0.40 V for PTV*c*BBO and PTV*t*BBO respectively. Overall, PTV*t*BBO-based PVCs had much better performance than PTV*c*BBO-based PVCs with a short-circuit current of 0.66 mA cm^{-2} and a fill factor of 31% (Fig. 4). In comparison, PTV*c*BBO-based PVCs had a short-circuit current of 0.12 mA cm^{-2} and a fill factor of 26%. These results are summarized in Table 3. The superior performance of PVCs based on PTV*t*BBO in comparison to PTV*c*BBO can be attributed to higher electron affinity and smaller band gap of PTV*t*BBO.

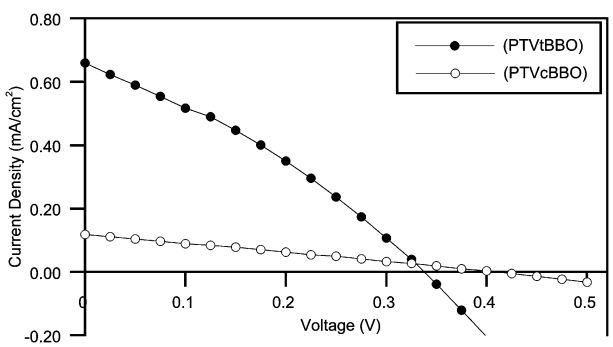

Fig. 3 Current–voltage characteristics of PTVBBO:PCBM photovoltaic cells.

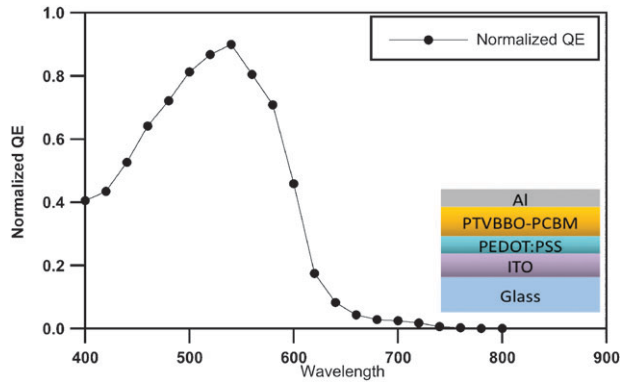

Fig. 4 Normalized quantum efficiency *vs.* wavelength curve of PTV*t*BBO:PCBM cells. Inset shows the device structure.

Table 3 Photovoltaic performance of PTVBBOs with PCBM

Polymer	V_{oc}/V	J_{sc}/mA cm^{-2}	FF (%)	PCE (%)
PTV*c*BBO	0.35	0.12	26	0.01
PTV*t*BBO	0.40	0.66	31	0.08

Polymers films were prepared from solutions in *o*-DCB 10 mg mL^{-1}.

While the performance of the PTV*t*BBO devices is lower than other state-of-the-art conjugated polymers, we note that these PVCs are the first to be fabricated from copolymers containing BBOs and thiophene. As a result, many processing parameters such as choice of solvent (or solvent mixtures), annealing, annealing temperatures, and polymer/PCBM ratios are not yet optimized. All of these parameters are critical, and their optimization alone has led to drastic improvements in the power conversion efficiencies of PVCs, based on other conjugated polymers such as rr-P3HT and poly[*N*-9′-heptadecanyl-2,7-carbazole-*alt*-5,5-(4′,7′-di-2-thienyl-2′,1′,3′-benzothiadiazole)] (PCDTBT). In part, the poor performance of the PVCs fabricated in this report can be ascribed to a non-optimal phase separation, as shown in the atomic force microscopy AFM phase image (ESI†). Aggregates of size 50–100 nm are observed, which are much larger than typical exciton diffusion lengths of conjugated polymers ($\sim$10 nm). Further evidence of the phase separation can be seen by Raman spectroscopy. When PTV*t*BBO film is more crystalline, the thiophene rings are, on average, more closely stacked. This should lead to narrowing of the peaks.[53,54] The spectra of the neat PTV*t*BBO film show peaks at 1560–1570, 1180 and 1230 cm^{-1}. In comparison, PTV*t*BBO:PCBM blend films exhibited broadening of these peaks which indicates a decrease in the crystallinity of PTVtBBO film. This loss of crystallinity can be attributed to very fine intermixing of PTVtBBO and PCBM domains, limiting the PTVtBBO crystallites to nanometre scale (ESI†). Such poor separation or nanoscale fine mixing of phases prevents the formation of continuous pathways for carrier transport to the electrodes, reducing the device efficiency. Although we could dissolve PTV*t*BBO in DCB, this solution does not pass through 0.2 micron filter as readily as solutions of rr-P3HT in DCB. This suggests that there are large aggregates of polymer in the solution. Thus improving the processibility of BBO polymers is expected to improve performance. Due to the superior performance of PVCs based on PTV*t*BBO in comparison to PTV*c*BBO, we evaluated the impact of solvent choice on the mobility of PTV*t*BBO. We first prepared thin films by dissolving PTV*t*BBO in four different solvents (*o*-dichlorobenzene, chlorobenzene, chloroform, and toluene), and the spun thin films from these solutions. We measured current-density–voltage (*J*–*V*) characteristics of hole-only diodes of these films and then extracted hole mobilities using the space-charge limited current (SCLC) model (ESI†). Not accounting for the electric field dependence of the SCLC model,[55–57] we found zero-field hole mobilities to be 1.76×10^{-5} cm^2 V^{-1} s^{-1} in chlorobenzene, 3.8×10^{-5} cm^2 V^{-1} s^{-1} in *o*-dichlorobenzene, 5.09×10^{-5} cm^2 V^{-1} s^{-1} in toluene, and 3.33×10^{-5} cm^2 V^{-1} s^{-1} in chloroform. These values are of the same order of magnitude as those reported in the literature for rr-P3HT using a similar hole-only diode architecture.[58,59] These results indicate that PTV*t*BBO is promising for use as an efficient hole transporter in PVCs.[50–52] Given its poor performance in PVCs, we did not evaluate the mobility of PTV*c*BBO.

Theoretical electronic structure calculations

To understand the difference in the performance between PTV*c*BBO and PTV*t*BBO we performed theoretical calculations using density functional theory. While the superior performance of PVCs based on PTV*t*BBO in comparison to PTV*c*BBO can be attributed to higher electron affinity and smaller band gap of PTV*t*BBO, the small difference between the two suggests that other factors are involved. The geometries of model oligomers (n = 1, 2, 3, and 4) for PTV*c*BBO and PTV*t*BBO were optimized at the density functional theory B3LYP/6-31G* level in which the didodecyl substituents were replaced with hydrogen atoms to reduce computational costs. The optimized geometries indicate that the model oligomers are planar, which should optimize conjugation and facilitate delocalization of electrons. The geometries of the model dimers indicated that the PTV*c*BBO structure had a much larger dipole moment (6.7 D) than that of the PTV*t*BBO (3.1 D). This phenomenon can be explained by the differences in the symmetry of the two BBOs. The *trans*-BBO moiety in the PTV*t*BBO molecule has three mirror planes and a center of inversion (C_{2h} point group) whereas the *cis*-BBO moiety in the PTV*c*BBO structure only possesses two mirror planes (C_{2v} point group). These symmetry differences could impact the electronic properties of the two polymers.

The HOMO, LUMO, band gap, and lowest lying singlet excited states (S_1) were computed at the TDDFT B3LYP/6-31G* and ZINDO/S[60] levels, respectively. Polymeric results were generated by fitting the aforementioned set of oligomers (n = 1, 2, 3, and 4) with the Kuhn expression[61,62]

$$E = E_0\sqrt{1 + 2\frac{k'}{k_0}\cos\frac{\pi}{N+1}} \qquad (1)$$

where E_0 is the transition energy of a formal double bond, N is the number of double bonds in the oligomer (thought to be identical oscillators), and k'/k_0 is an adjustable parameter (indicative of the strength of coupling between the oscillators).

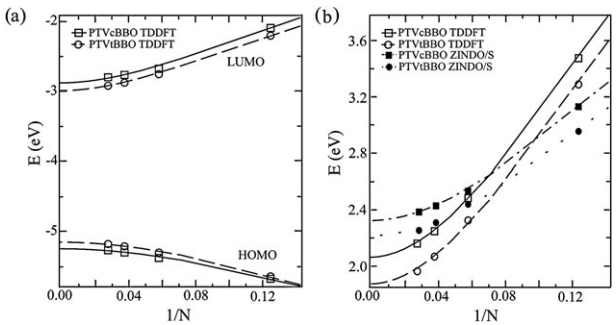

Fig. 5 Kuhn fits for (a) HOMOs, LUMOs (TDDFT level) and (b) band gaps, E_g (TDDFT level), and first excited states, S_1 (ZINDO/S level), for PTV*c*BBO and PTV*t*BBO.

These fits were performed on both sets of data and are shown in Fig. 5. The results of these fits are summarized in Table 4.

The computational results for the HOMO and LUMO show relatively good agreement with experimental values. The band gaps obtained at the DFT level are significantly underestimated which is a consequence of the overestimation of the chain-length dependence of the transition energies.[61] However, they are comparable in deviation from experiment as the ZINDO results whose level of theory was parameterized to reproduce the band gaps for a large number of compounds in apolar solvents.[60] In either case these results confirm that electronic properties of PTV*c*BBO and PTV*t*BBO are different as suggested by their point groups. While PTV*t*BBO has a higher HOMO, a lower LUMO and thus a smaller band gap than PTV*c*BBO, neither polymer has a high enough LUMO for use as an acceptor polymer with rr-P3HT as the donor in PVCs.

The HOMO and LUMO wavefunctions for model dimers ($n = 2$) of PTV*c*BBO and PTV*t*BBO are shown in Fig. 6 along with the wavefunction for an oligomer ($n = 8$) of rr-P3HT whose hexyl groups have been replaced with methyl groups to reduce computational cost. In all cases the HOMO wavefunction is delocalized along the entire dimer. In contrast, the LUMO wavefunctions for PTV*c*BBO and PTV*t*BBO illustrate that the electron density of these materials is centered on the thiophene moieties, instead of being localized on the electron-accepting BBO subunits. This is the opposite of what is commonly seen in polymers which possess alternating donor and acceptor subunits.[43,63,64] In these polymers the electron density of the LUMO is localized on the electron accepting group. The fact that the LUMO wavefunction for PTV*c*BBO and PTV*t*BBO is localized on the thiophene moieties justifies the PVC results in that (1) the frontier orbitals demonstrate a similar localization as is found in P3HT, leading to electron donating rather than electron accepting behavior in this system;[65] (2) the LUMO wavefunction of PTV*t*BBO is more delocalized than that of PTV*c*BBO, in that more density is located on the acceptor moiety, elucidating the origin of better performance in the PVCs; (3) the lesser extent of delocalization in the LUMO wavefunction of PTV*t*BBO in comparison to that of rr-P3HT explains why the performance of PTV*t*BBO was not as good as rr-P3HT despite the higher LUMO level. Thus the development of new polymers which exhibit a higher degree of delocalization from the donor moieties to the BBO moiety in the LUMO could result in improved performance in PVCs.

Table 4 HOMO and LUMO orbital energies, band gaps, and energies of the lowest lying singlet excited states in eV derived from the Kuhn fits of the two data sets with percent error relative to experiment in parentheses

	HOMO[a]	LUMO[a]	E_g[a]	S_1[b]
PTV*c*BBO	−5.25 (1.2%)	−2.88 (4.6%)	2.06 (5.1%)	2.32 (6.9%)
PTV*t*BBO	−5.16 (0.4%)	−2.99 (3.5%)	1.87 (9.1%)	2.22 (8.8%)

[a] Computed from TDDFT B3LYP/6-31G* level. [b] Computed from the ZINDO/S level.

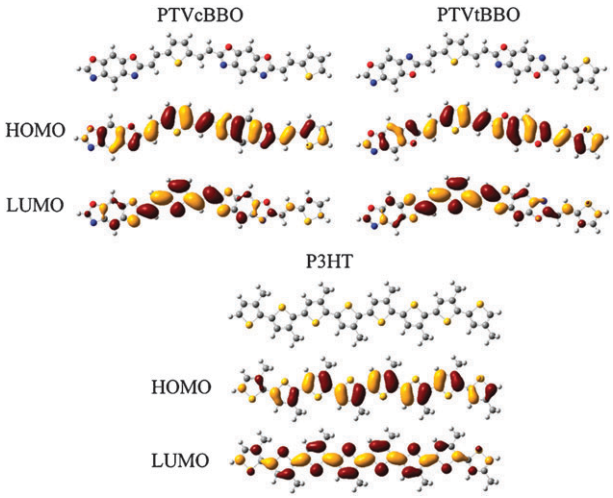

Fig. 6 HOMO and LUMO frontier orbitals of the PTV*c*BBO, and PTV*t*BBO dimers and P3HT oligomer, obtained at the DFT B3LYP/6-31G* level.

Conclusions

In conclusion two new organic-soluble, thiophene–BBO copolymers have been synthesized. Both polymers show reversible reduction, while PTV*t*BBO behaved as a donor in bulk heterojunction PVCs with PCBM. DFT calculations reveal that both polymers have high electron affinities, but poor delocalization in the LUMO wavefunction. Thus, while the polymers were designed to be a D–A system, the thiophene rings do not donate electron density to the BBO moieties. The narrow band gap, low lying LUMO and reversible electrochemistry of these polymers suggest that BBOs are useful building blocks for the synthesis of conjugated polymers. Future research will focus on increasing the extent of delocalization in these polymers.

Experimental section

The monomers 2,6-dimethylbenzo[1,2-d;5,4-d′]bisoxazole-diethylphosphonate ester,[37] 2,6-dimethylbenzo[1,2-d;4,5-d′]bisoxazole-diethylphosphonate ester[38] and 3,4-didodecylthiophene-2,5-dicarboxaldehyde[42] were all synthesized according to the previously reported methods. Tetrahydrofuran was dried using an Innovative Technologies solvent purification system.

All other compounds were purchased from commercial sources and used without further purification. Nuclear magnetic resonance spectra were obtained on a Varian 400 MHz spectrometer. All samples were referenced internally to the residual protonated solvent and the chemical shifts are given in δ, relative to the solvent. Gel permeation chromatography (GPC) measurements were performed on a Viscotek GPC Max 280 separation module equipped with three 5 μm I-gel columns connected in a series (guard, HMW, MMW and LMW) with a refractive index detector. Analyses were performed at 35 °C using THF as the eluent with the flow rate at 1.0 mL min^{-1}. Calibration was based on polystyrene standards. Fluorescence spectroscopy and UV-Visible spectroscopy were obtained using polymer solutions in THF, and thin films were spun from these solutions. Both polymers were excited at their respective emission maxima. Thermal gravimetric analysis measurements were performed using TA instruments Model Q50, within the temperature interval of 30 °C–650 °C, with a heating rate of 20 °C per minute, under ambient atmosphere. Cyclic voltammograms were performed in 0.1 M tetrabutylammonium hexafluorophosphate using 0.01 M $AgNO_3$ in the acetonitrile reference electrode. The potential values obtained *versus* the Ag^+ were converted to the ferrocene (Fc) reference.

General methods for polymer synthesis

We dissolved the BBO monomer (460 mg, 1.00 mmol) and 3,4-didodecylthiophene (503 mg, 1.00 mmol) in 15 mL of THF. Then we added a 1 M solution of potassium *tert*-butoxide in THF (2.5 mL, 2.5 mmol) to the solution and the mixture, and we stirred the solution at room temperature for 48 h to obtain an opaque, dark red solution. Then we added an additional 10 mL of THF and stirred the reaction for an additional 72 h. We then precipitated the solution by pouring it into MeOH and collected the resulting red-orange solid by filtration. We purified the polymer *via* Soxhlet extraction washing first with MeOH for 8 h, followed by hexane for 8 h and lastly THF for 8 h. The polymer was obtained upon evaporation of the THF solution.

PTV*c*BBO (78% yield). ^{1}H-NMR (400 MHz, THF-d_8): δ 0.89 (m, CH_3-), 1.30 (br m, -$(CH_2)_4$-), 2.39–2.77 (br m, -Ar-CH_2-), 6.19, 7.75 (br s, vinylic peaks), 7.85 and 7.95 (br s, Ar-H).

PTV*t*BBO (87% yield). ^{1}H-NMR (400 MHz, THF-d_8): δ 0.89 (m, CH_3-), 1.30 (br m, -$(CH_2)_4$-), 2.79–2.95 (br m, -Ar-CH_2-), 6.91, 7.79 (br s, vinylic peaks), 7.98 (br m, Ar-H).

Fabrication and characterization of polymer solar cells

Photovoltaic cells were fabricated from quartz slides coated with indium tin oxide (ITO) (Delta Technologies Inc.,). The slides were then cleaned by sonication in acetone, isopropanol, detergent, and de-ionized water. The slides were then dried under nitrogen and exposed to air plasma for one minute. Poly(3,4-ethylenedioxythiophene) (PEDOT:PSS) (Clevios P™) was filtered through a 0.45 μm and spin-coated (600 rpm for 60 s) onto the slides to serve as a hole transport layer. The slides were then dried on a hot plate at 120 °C for 10 min. After cooling, the slides were transferred to a glove box with an Ar atmosphere. PTV*t*BBO and PTV*c*BBO were mixed with PCBM (Sigma Aldrich) in 1 : 1 weight ratio. Total solute concentration in all solutions was 20 mg ml^{-1}. *o*-DCB was the solvent used for PVCs and hole-mobility measurements. Additionally, chloroform, toluene and chlorobenzene were also used for mobility measurements. All active-layer solutions were passed through 0.22 μm PTFE syringe filters (Whatman) and spin coated on the PEDOT:PSS layer at 600 rpm for 60 s. The samples were then dried in a Petri dish. Finally, aluminium electrode (100 nm) was thermally evaporated for PVCs, and gold electrode (100 nm) was evaporated in an E-beam evaporator for hole-mobility measurements. The area of metal electrode for both types of devices was 4 mm^2.

The current density–voltage (*I–V*) characteristics of the PVCs and hole-only diodes were measured using a Keithley 276 source-measurement unit and a HP 4156A semiconductor parameter analyzer, respectively. The PVCs were illuminated through the ITO side using a GE ELH bulb, the intensity of which was adjusted to 100 mW cm^{-2} using a crystalline silicon reference cell.

For optical measurements, solutions were spin-coated onto quartz slides to form active layers. The optical absorption spectra of these films were recorded using a UV-VIS spectrophotometer (Cary 50 Bio). The steady state PL spectra were measured using a Spex Fluorolog Tau-3 fluorescence spectrophotometer.

Theoretical calculations

All of the calculations on these oligomers were studied using the Gaussian 03W[66] program package with the GaussView 4 GUI interface program package. The electronic ground states were optimized using density functional theory (DFT), B3LYP/6-31G*. Excited states were generated through time dependent density functional theory (TD-DFT) applied to the optimized ground state for each oligomer. The HOMO, LUMO, band gap, first ten excited states, frontier orbitals and UV-Vis simulations were generated from these excited computations. Finally, electrostatic potential maps were created using a coarse setting and an isovalue of 0.03.

Acknowledgements

This work was funded by the National Science Foundation (DMR-0846607), the 3M foundation, and the Iowa Office of Energy Independence through the Iowa Power Fund. The device fabrication and characterization was performed at the Iowa State University Microelectronics Research Center. We thank Mr Robert Roggers (ISU) for X-ray analysis and Ms Kimberly Topp (ISU) for help with the abstract graphic.

Notes and references

1 K. M. Coakley and M. D. McGehee, *Chem. Mater.*, 2004, **16**, 4533–4542.
2 B. C. Thompson and J. M. J. Frechet, *Angew. Chem., Int. Ed.*, 2008, **47**, 58–77.
3 B. C. Thompson, Y.-G. Kim and J. R. Reynolds, *Macromolecules*, 2005, **38**, 5359–5362.
4 L. J. A. Koster, V. D. Mihailetchi and P. W. M. Blom, *Appl. Phys. Lett.*, 2006, **88**, 093511–093513.

5 L. J. A. Koster, V. D. Mihailetchi, R. Ramaker and P. W. M. Blom, *Appl. Phys. Lett.*, 2005, **86**, 123509–123512.
6 C. J. Brabec, A. Cravino, D. Meissne, N. S. Sariciftci, T. Fromherz, M. T. Rispens, L. Sanchez and J. C. Hummelen, *Adv. Funct. Mater.*, 2001, **11**, 374–380.
7 E. Bundgaard and F. C. Krebs, *Sol. Energy Mater. Sol. Cells*, 2007, **91**, 954–985.
8 C. Winder and N. S. Sariciftci, *J. Mater. Chem.*, 2004, **14**, 1077–1086.
9 H. A. M. van Mullekom, J. A. J. M. Vekemans, E. E. Havinga and E. W. Meijer, *Mater. Sci. Eng., R*, 2001, **32**, 1–40.
10 S. A. Jenekhe, L. Lu and M. M. Alam, *Macromolecules*, 2001, **34**, 7315–7324.
11 J. Mei, N. C. Heston, S. V. Vasilyeva and J. R. Reynolds, *Macromolecules*, 2009, **42**, 1482–1487.
12 M. Jeffries-El and R. D. McCullough, in *Handbook of Conducting Polymers*, ed. T. A. Skotheim and John R. Reynolds, London, Boca Raton, FL, 3rd edn, 2007, pp. 331–380.
13 R. D. McCullough, in *Handbook of Conducting Polymers*, ed. T. A. Skotheim, Ronald L. Elsenbaumer and John R. Reynolds, Marcell Dekker, New York, 2nd edn, 1998, pp. 225–258.
14 J. Liu, R. Zhang, G. Sauve, T. Kowalewski and R. D. McCullough, *J. Am. Chem. Soc.*, 2008, **130**, 13167–13176.
15 Y. Li, L. Xue, H. Li, Z. Li, B. Xu, S. Wen and W. Tian, *Macromolecules*, 2009, **42**, 4491–4499.
16 E. Ahmed, F. S. Kim, H. Xin and S. A. Jenekhe, *Macromolecules*, 2009, **42**, 8615–8618.
17 J. F. Wolfe, *Encyclopedia of Polymer Science and Engineering*, John Wiley and Sons, New York, NY, 1988, vol. 11, pp. 601–635.
18 J. F. Wolfe and F. E. Arnold, *Macromolecules*, 1981, **14**, 909–915.
19 M. M. Alam and S. A. Jenekhe, *Chem. Mater.*, 2002, **14**, 4775–4780.
20 S. A. Jenekhe, L. R. de Paor, X. L. Chen and R. M. Tarkka, *Chem. Mater.*, 1996, **8**, 2401–2404.
21 Y. Chen, S. Wang, Q. Zhuang, X. Li, P. Wu and Z. Han, *Macromolecules*, 2005, **38**, 9873–9877.
22 D. Feng, S. Wang, Q. Zhuang, P. Wu and Z. Han, *Polymer*, 2004, **45**, 8871–8879.
23 S. A. Jenekhe and J. A. Osaheni, *Chem. Mater.*, 1994, **6**, 1906–1909.
24 J. A. Osaheni and S. A. Jenekhe, *Macromolecules*, 1994, **27**, 739–742.
25 J. A. Osaheni and S. A. Jenekhe, *Chem. Mater.*, 1995, **7**, 672–682.
26 J. A. Osaheni, S. A. Jenekhe, A. Burns, G. Du, J. Joo, Z. Wang, A. J. Epstein and C. S. Wang, *Macromolecules*, 1992, **25**, 5828–5835.
27 X. Zhang and S. A. Jenekhe, *Macromolecules*, 2000, **33**, 2069–2082.
28 L.-S. Tan, J. L. Burkett, S. R. Simko and M. D. Alexander, Jr., *Macromol. Rapid Commun.*, 1999, **20**, 16–20.
29 S. Wang, Y. Chen, Q. Zhuang, X. Li, P. Wu and Z. Han, *Macromol. Chem. Phys.*, 2006, **207**, 2336–2342.
30 S. Wang, P. Guo, P. Wu and Z. Han, *Macromolecules*, 2004, **37**, 3815–3822.
31 S. Wang, H. Lei, P. Guo, P. Wu and Z. Han, *Eur. Polym. J.*, 2004, **40**, 1163–1167.
32 P. Guo, S. Wang, P. Wu and Z. Han, *Polymer*, 2004, **45**, 1885–1893.
33 H. R. Kricheldorf and A. Domschke, *Polymer*, 1994, **35**, 198–203.
34 X. Liu, X. Xu, Q. Zhuang and Z. Han, *Polym. Bull.*, 2008, **60**, 765–774.
35 Y. Imai, K. Itoya and M.-A. Kakimoto, *Macromol. Chem. Phys.*, 2000, **201**, 2251–2256.
36 Y. So, J. P. Heeschen, B. Bell, P. Bonk, M. Briggs and R. DeCaire, *Macromolecules*, 1998, **31**, 5229–5239.
37 J. F. Mike, A. J. Makowski and M. Jeffries-EL, *Org. Lett.*, 2008, **10**, 4915–4918.
38 J. F. Mike, A. J. Makowski, T. C. Mauldin and M. Jeffries-El, *J. Polym. Sci., Part A: Polym. Chem.*, 2010, **48**, 1456–1460.
39 P. M. Beaujuge, S. V. Vasilyeva, S. Ellinger, T. D. McCarley and J. R. Reynolds, *Macromolecules*, 2009, **42**, 3694–3706.
40 J. Roncali, *Chem. Rev.*, 1997, **97**, 173–205.
41 D. A. M. Egbe, C. P. Roll, E. Birckner, U.-W. Grummt, R. Stockmann and E. Klemm, *Macromolecules*, 2002, **35**, 3825–3837.
42 S. Destri, M. Pasini, C. Pelizzi, W. Porzio, G. Predieri and C. Vignali, *Macromolecules*, 1999, **32**, 353–360.
43 E. Zhou, M. Nakamura, T. Nishizawa, Y. Zhang, Q. Wei, K. Tajima, C. Yang and K. Hashimoto, *Macromolecules*, 2008, **41**, 8302–8305.
44 E. Zhou, K. Tajima, C. Yang and K. Hashimoto, *J. Mater. Chem.*, 2010, **20**, 2362–2368.
45 J. J. M. Halls, J. Cornil, D. A. dos Santos, R. Silbey, D. H. Hwang, A. B. Holmes, J. L. BrÈdas and R. H. Friend, *Phys. Rev. B: Condens. Matter Mater. Phys.*, 1999, **60**, 5721.
46 S. Barth and H. Bassler, *Phys. Rev. Lett.*, 1997, **79**, 4445.
47 B. Friedel, C. R. McNeill and N. C. Greenham, *Chem. Mater.*, 2010, **22**, 3389–3398.
48 M. Scharber, D. Mühlbacher, M. Koppe, P. Denk, C. Waldauf, A. Heeger and C. Brabec, *Adv. Mater.*, 2006, **18**, 789–794.
49 J. Y. Kim, K. Lee, N. E. Coates, D. Moses, T.-Q. Nguyen, M. Dante and A. J. Heeger, *Science*, 2007, **317**, 222–225.
50 G. Li, V. Shrotriya, J. Huang, Y. Yao, T. Moriarty, K. Emery and Y. Yang, *Nat. Mater.*, 2005, **4**, 864–868.
51 J. Y. Kim, S. H. Kim, H.-H. Lee, K. Lee, W. Ma, X. Gong and A. J. Heeger, *Adv. Mater.*, 2006, **18**, 572–576.
52 S. H. Park, A. Roy, S. Beaupre, S. Cho, N. Coates, J. S. Moon, D. Moses, M. Leclerc, K. Lee and A. J. Heeger, *Nat. Photonics*, 2009, **3**, 297–302.
53 J. Casado, R. G. Hicks, V. Hernandez, D. J. T. Myles, M. C. Ruiz Delgado and J. T. Lopez Navarrete, *J. Chem. Phys.*, 2003, **118**, 1912–1920.
54 E. Klimov, W. Li, X. Yang, G. G. Hoffmann and J. Loos, *Macromolecules*, 2006, **39**, 4493–4496.
55 C. Tanase, P. W. M. Blom and D. M. De Leeuw, *Phys. Rev. B: Condens. Matter Mater. Phys.*, 2004, **70**, 193202.
56 P. N. Murgatroyd, *J. Phys. D: Appl. Phys.*, 1970, **3**, 151–157.
57 M. A. Lampert, A. Many and P. Mark, *Phys. Rev.*, 1964, **135**, A1444–A1453.
58 O. G. Reid, K. Munechika and D. S. Ginger, *Nano Lett.*, 2008, **8**, 1602–1609.
59 C. Goh, R. J. Kline, M. D. McGehee, E. N. Kadnikova and J. M. J. Frechet, *Appl. Phys. Lett.*, 2005, **86**, 122110–122113.
60 A. Hartman and M. C. Zerner, *Theor. Chim. Acta*, 1975, **37**, 47–65.
61 J. Gierschner, J. Cornil and H.-J. Egelhaaf, *Adv. Mater.*, 2007, **19**, 173–191.
62 B. Milian Medina, A. VanVooren, P. Brocorens, J. Gierschner, M. Shkunov, M. Heeney, I. McCulloch, R. Lazzaroni and J. Cornil, *Chem. Mater.*, 2007, **19**, 4949–4956.
63 X. Zhang, T. T. Steckler, R. R. Dasari, S. Ohira, W. J. Potscavage Jr, S. P. Tiwari, S. Coppee, S. Ellinger, S. Barlow, J.-L. Bredas, B. Kippelen, J. R. Reynolds and S. R. Marder, *J. Mater. Chem.*, 2010, **20**, 123–134.
64 B. P. Karsten, L. Viani, J. Gierschner, J. Cornil and R. A. J. Janssen, *J. Phys. Chem. A*, 2008, **112**, 10764–10773.
65 M. Chen, X. Crispin, E. Perzon, M. R. Andersson, T. Pullerits, M. Andersson, O. Inganas and M. Berggren, *Appl. Phys. Lett.*, 2005, **87**, 252105–252103.
66 M. J. T. Frisch, G. W. Trucks, H. B. Schlegel, G. E. Scuseria, M. A. Robb, J. R. Cheeseman, J. A. Montgomery, Jr., T. Vreven, K. N. Kudin, J. C. Burant, J. M. Millam, S. S. Iyengar, J. Tomasi, V. Barone, B. Mennucci, M. Cossi, G. Scalmani, N. Rega, G. A. Petersson, H. Nakatsuji, M. Hada, M. Ehara, K. Toyota, R. Fukuda, J. Hasegawa, M. Ishida, T. Nakajima, Y. Honda, O. Kitao, H. Nakai, M. Klene, X. Li, J. E. Knox, H. P. Hratchian, J. B. Cross, V. Bakken, C. Adamo, J. Jaramillo, R. Gomperts, R. E. Stratmann, O. Yazyev, A. J. Austin, R. Cammi, C. Pomelli, J. W. Ochterski, P. Y. Ayala, K. Morokuma, G. A. Voth, P. Salvador, J. J. Dannenberg, V. G. Zakrzewski, S. Dapprich, A. D. Daniels, M. C. Strain, O. Farkas, D. K. Malick, A. D. Rabuck, K. Raghavachari, J. B. Foresman, J. V. Ortiz, Q. Cui, A. G. Baboul, S. Clifford, J. Cioslowski, B. B. Stefanov, G. Liu, A. Liashenko, P. Piskorz, I. Komaromi, R. L. Martin, D. J. Fox, T. Keith, M. A. Al-Laham, C. Y. Peng, A. Nanayakkara, M. Challacombe, P. M. W. Gill, B. Johnson, W. Chen, M. W. Wong, C. Gonzalez and J. A. Pople, *Gaussian 03, revision C.02*, Gaussian Inc., Wallingford, CT, 2004.

